Observation of Topological Phase Transitions in Photonic Quasicrystals

Mor Verbin,[1] Yaacov E. Kraus,[2] Oded Zilberberg,[2] Yoav Lahini,[1,3] and Yaron Silberberg[1]

[1] *Department of Physics of Complex Systems, Weizmann Institute of Science, Rehovot 76100, Israel.*
[2] *Department of Condensed Matter Physics, Weizmann Institute of Science, Rehovot 76100, Israel.*
[3] *Department of Physics, Massachusetts Institute of Technology, Cambridge MA, USA.*

Topological insulators and topological superconductors are distinguished by their bulk phase transitions and gapless states at a sharp boundary with the vacuum. Quasicrystals have recently been found to be topologically nontrivial. In quasicrystals, the bulk phase transitions occur in the same manner as standard topological materials, but their boundary phenomena are more subtle. In this work we directly observe bulk phase transitions, using photonic quasicrystals, by constructing a smooth boundary between topologically-distinct one-dimensional quasicrystals. Moreover, we use the same method to experimentally verify the topological equivalence between the Harper and Fibonacci quasicrystals.

PACS numbers: 71.23.Ft, 73.43.-f, 73.43.Nq, 05.30.Rt

The classification of gapped systems, such as band insulators and superconductors, by topological indices is a rapidly developing paradigm in condensed matter physics [1, 2]. This novel approach provides insights to the characterization of states of matter, as well as predicts exotic phenomena.

The topological classification of a system assigns an integer index to its energy gap. This index encodes properties that are robust to distortions and deformation of the system. Hence, when a system with a given index is continuously deformed into a system whose index has a different value, the bulk energy gap must close, namely a quantum phase transition occurs. Accordingly, if a system can be continuously deformed into another system while keeping the bulk gap open, then their topological indices must be the same, defining them as topologically equivalent. Usually, such a phase transition manifests by the appearance of gap-traversing states at the boundary between topologically nontrivial materials and the topologically-trivial vacuum. Examples for such boundary states are the chiral modes of the integer quantum Hall effect (IQHE), the Dirac cone of the three-dimensional topological insulator, and the Majorana fermions of one-dimensional (1D) topological superconductors [1, 2].

There is a variety of realizations to these exciting systems in condensed matter, such as semiconducting heterostructures [3, 4], Bismuth-based compounds [5–7], and InSb nano-wires [8–10]. Additional instances were observed in photonic crystals [11, 12], and suggested to appear in cold atoms [13].

A new type of topological phenomena has been recently studied in quasiperiodic systems [14, 15]. Such systems, which are ordered but not periodic, were shown to be characterized by topological indices that are usually attributed to systems of a dimension higher than their physical dimension. In particular, it was shown that the canonical 1D quasiperiodic systems, i.e. the Harper (or Aubry-André) model [16, 17], the diagonal Fibonacci model [18, 19], and their quasicrystalline off-diagonal variants [20, 21], can be assigned Chern numbers. These number are topological indices that characterize generic two-dimensional (2D) systems [14, 15]. A continuous deformation between two quasicrystals (QCs) with different Chern numbers will therefore result in a bulk phase transition. Correspondingly, at a sharp boundary between such a QC and the vacuum, localized subgap boundary states may appear. These states were experimentally observed in photonic Harper QCs [14]. Further analyses of 1D topological QCs with sharp boundaries have been conducted in cold atoms [22, 23] and superconducting wires [24–28].

The topological characterization of a QC is based on its long-range order, which is broken at the sharp boundary. Therefore, these boundary states do not always appear. However, if the boundary between the nontrivial QC and the trivial vacuum is formed by an adiabatic deformation, subgap states will always appear at the boundary, revealing the bulk gap closure. Accordingly, such a deformation can be used to prove equivalence between different quasiperiodic systems, if the energy gap remains open throughout the deformation.

In this letter, we study the bulk gap closure that occurs when continuously deforming between topologically inequivalent quasiperiodic systems, and its absence when the systems are topologically equivalent. To this end, we create two inequivalent Harper QCs, and spatially interpolate between them. We then observe the closure of bulk energy gaps through the emergence of subgap states localized within the deformation region. In contrast, using the same interpolation process between seemingly different but topologically equivalent systems, the Harper and the Fibonacci QCs, no such phase transition occurs, thereby proving that these two models are indeed topologically equivalent. These phenomena are experimentally tested in quasiperiodic photonic lattices, where the phase transition, or its absence, are directly observed using the propagation of light in waveguide arrays.

Photonic lattices are widely used for realizations of different models originating from solid state physics, due to the high level of control over their parameters and behavior [29, 30]. Our photonic QCs are composed of an array of coupled single-mode waveguides, fabricated in bulk glass using femtosecond laser micro-fabrication technology [31, 32]. The overlap between the evanescent modes of the waveguides allows the propagating light to tunnel from each waveguide to its neighboring waveguides. Hence, the hopping amplitude between adjacent waveguides can be controlled by modulating the spacing between them.

The dynamics of light propagating in these coupled waveguide arrays is described by the tight-binding model, with the propagation axis z taking over the role of time, $i\partial_z\psi_n = H\psi_n$, where ψ_n is the wavefunction at waveguide number n. Taking the hopping amplitude to be real, we obtain the general Hamiltonian

$$H\psi_n = t_n\psi_{n-1} + t_{n+1}\psi_{n+1}\,, \tag{1}$$

where t_n is the hopping amplitude from site n to site $n-1$.

Our intention is to study the transition that occurs when some system I is deformed into another system II, where each system has its own set of quasiperiodic hopping amplitudes t_n^I and t_n^{II}, respectively. To this end, we fabricate a waveguide array with a deformed hopping profile $t_n = f_n t_n^I + (1-f_n)\, t_n^{II}$, where

$$f_n = \begin{cases} 1 & 1 \le n \le L_I \\ 1 - \frac{n-L_I}{L_D} & L_I < n < L_I + L_D \\ 0 & L_I + L_D \le n \le L_I + L_D + L_{II} \end{cases}, \tag{2}$$

as depicted in Fig. 1(a). This procedure produces an array of length L_I of system I on one side of the structure, an array of length L_{II} of system II on the other side, and an L_D-long deformation region, which continuously transforms between the two. This structure enables the study of the eigenstates of both systems as well as the transition between them, on a single waveguide array.

The properties of the Hamiltonian fabricated within the photonic crystal are studied by injecting light into one of the waveguides in the array and measuring the outgoing intensity at the output facet using a CCD camera, as illustrated in Fig. 1(b). The injected beam excites a wavepacket of all the modes that have a non-vanishing amplitude at the injection site, and the light propagates in the lattice according to this superposition of eigenstates. The width of the outgoing intensity distribution can therefore reveal the existence of localized eigenstates: If there is no localized state near the injection site, the light will spread freely throughout the array, propagating according to the bulk properties of the system. However, when light is injected in the vicinity of a localized state, its expansion is regulated by the width of the state. To

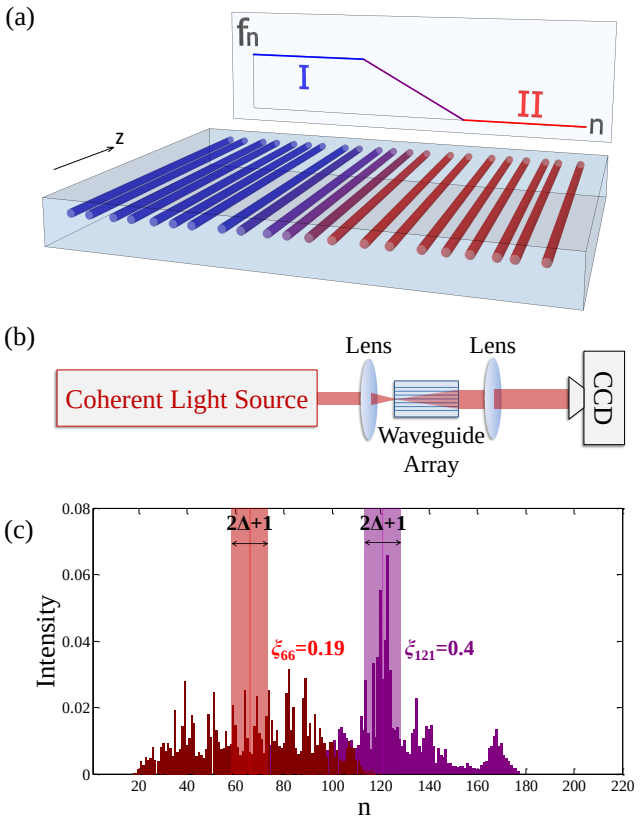

FIG. 1. (Color online) Experimental methods. (a) Illustration of a photonic waveguide array implementing a deformation between two QCs [cf. Eq. (2)]. (b) A schematics of the experimental setup. We focus a coherent light beam into a waveguide in the array, allow it to propagate along the structure, and image the output intensity using a CCD camera. (c) Illustration of the relation between the localization parameter ξ_n and the measured intensity distribution $|\psi_n|^2$ for two injection sites, $n = 66$ and $n = 121$. The shaded intervals denote the Δ-distance neighborhood around the insertion point. When more light remains within this neighborhood, the value of ξ_n increases.

quantify the localization of the outgoing light, we measure the amount of light that remains within a small distance Δ from the injection site n, by measuring the generalized return probability [33],

$$\xi_n = \Big(\sum_{m=n-\Delta}^{n+\Delta} |\psi_m|^2\Big) \Big/ \Big(\sum_{m=1}^{L_I+L_D+L_{II}} |\psi_m|^2\Big)\,. \tag{3}$$

The relation between ξ_n and the intensity distribution $|\psi_n|^2$ is illustrated in Fig. 1(c). Since ξ_n is meant to reveal the existence of localized states, we will choose Δ to be of the order of the width of a localized subgap state.

Let us now introduce the specific quasiperiodic tight-binding models under study. In these models the hopping amplitude is modulated according to

$$t_n = t_0\,[1 + \lambda d_n]\,, \tag{4}$$

where t_0 is the characteristic hopping amplitude of the system, $\lambda \in [0,1)$ is the modulation strength, and $d_n \in [-1,1]$ is some quasiperiodic modulation function.

Here we consider two such modulations: the Harper modulation

$$d_n^{\mathrm{H}} = \cos(2\pi b n + \phi)\,, \tag{5}$$

and the Fibonacci-like modulation

$$d_n^{\mathrm{F}} = 2\left(\left\lfloor \frac{\tau}{\tau+1}(n+2)\right\rfloor - \left\lfloor \frac{\tau}{\tau+1}(n+1)\right\rfloor\right) - 1 = \pm 1\,. \tag{6}$$

The long-range order of the Harper QC [20] is controlled by the modulation frequency b. Whenever b is irrational, the hopping modulation is incommensurate with the underlying lattice, resulting in a quasiperiodic pattern. The parameter ϕ shifts the origin of the modulation. The energy spectrum of the Harper model is composed of a fractal set of bands and gaps, in a way that depends on the modulation frequency b [20, 34]. Moreover, these gaps are associated with Chern numbers uniquely determined by b [15, 35]. Hence, two Harper QCs with $b_I \neq b_{II}$ are typically topologically inequivalent, since their gaps are associated with different Chern numbers. Comparably, the Fibonacci-like QC is constructed from a sequence of two values that are ordered in a quasiperiodic manner. This sequence is obtained by applying the "cut-and-project" procedure on a square lattice onto the line $y = x/\tau$ [36]. Whenever the slope of the line, τ, is irrational, the sequence is quasiperiodic. For example, the case of $\tau = (1+\sqrt{5})/2$ is the well-known Fibonacci QC [36, 37].

The properties of the Fibonacci-like QC differ in many ways from those of the Harper QC, e.g. the localization of the bulk wavefunctions [18–21, 38, 39]. Nevertheless, it was recently proven that they are topologically equivalent whenever the frequency of the Harper modulation satisfies $b = (\tau+1)/\tau$ [15]. In such a case, the gaps of the Fibonacci-like QC are associated with the same Chern numbers as those of the Harper QC. Hence, for a given modulation frequency b, the Harper QC can be continuously deformed into the Fibonacci-like QC without the appearance of a phase transition.

Note that the deformation in Eq. (5) contains an addition degree of freedom in the form of the parameter ϕ. This parameter has a crucial role in the observation of the topological boundary states of quasiperiodic systems [14]. While the spectrum of our model is gapped in the bulk, localized boundary states appear, which traverse the energy gaps as a function of ϕ. Nevertheless, in this work we focus on bulk properties, which are ϕ-independent [40].

We now turn to our experimental results. We construct a deformation between topologically inequivalent Harper QCs with modulation frequencies $b_I \neq b_{II}$. Figure 2(a) depicts the hopping amplitudes of a deformation between a Harper QC with $b_I = 2/(1+\sqrt{5})$ and a Harper QC with $b_{II} = 2/(1+\sqrt{6.5})$, where $t_0 = 28/75$ mm^{-1}, $\lambda = 0.475$ and $\phi_I = \phi_{II} = \pi$. The region lengths were taken to be $L_I = L_{II} = 84$ and $L_D = 51$. For this set of parameters, the bulk wavefunctions of the Harper QCs are extended [20]. We fabricated this structure in a 75mm-long photonic waveguide array. This results in an effective propagation of 14 tunneling lengths, where the tunneling length is the characteristic length for hopping, namely $2/t_0$. With such a propagation length, light injected in the bulk of the structure will sufficiently expand in comparison to the width of localized subgap states.

To experimentally observe the phase transition between the two QCs, we injected light into each waveguide, and measured ξ_n as a function of the injection point n. The results are presented in Fig. 2(b). Two clear peaks in the deformation region can be seen over a relatively flat ξ_n outside the region. This is a clear indication of the existence of localized states within the deformation region. Note that measurements of ξ_n for $n < 30$ and $n > 190$ are omitted from this plot – for these injection sites the expanding light hits the edges of the structure, causing ξ_n to be skewed by boundary effects.

To reveal the source of the peaks observed in ξ_n, we numerically obtain the local density of states (LDOS), which is presented in Fig. 2(c). The LDOS is defined by $D_n(E) = \sum_m \delta(E - E_m)\left|\varphi_n^{(m)}\right|^2$, where E_m is the energy of the m^{th} eigenstates, and $\varphi_n^{(m)}$ is its wavefunction. $D_n(E)$ describes the spatial distribution of the eigenstates of the structure as a function of energy. For $n \leq L_I$, we observe bands of extended states that correspond to the eigenstates of system I. Similarly, for $n \geq L_I + L_D$ we recognize the band of extended states of system II. However, within the deformation region, there are few states that reside within the energy gaps and are spatially localized. These localized states traverse the energy gap along the deformation region, are an explicit signature of the phase transition between the inequivalent QCs [40], and are the origin of the measured peaks in ξ_n. We have therefore experimentally observed the bulk phase transition between two topologically inequivalent Harper QCs.

We now turn to study the transition between topologically equivalent QCs. We constructed a deformation between a Harper QC and Fibonacci QC, with a matched modulation frequency $b_I = (\tau_{II}+1)/\tau_{II} = 2/(1+\sqrt{5})$ [41]. The hopping amplitudes t_n are depicted in Fig. 2(d), for $t_0 = 28/75$ mm^{-1}, $\lambda = 0.225$, $\phi = \pi(1+3b)$, $L_I = L_{II} = 84$ and $L_D = 51$. For this set of parameters, the bulk wavefunctions of the Harper QC are extended, while those of the Fibonacci are critical [21]. Nevertheless, for the structure's effective propagation length, light injected into the bulk of both QCs will sufficiently expand in comparison to the width of potential localized states. The measured ξ_n of this system is depicted in Fig. 2(e),

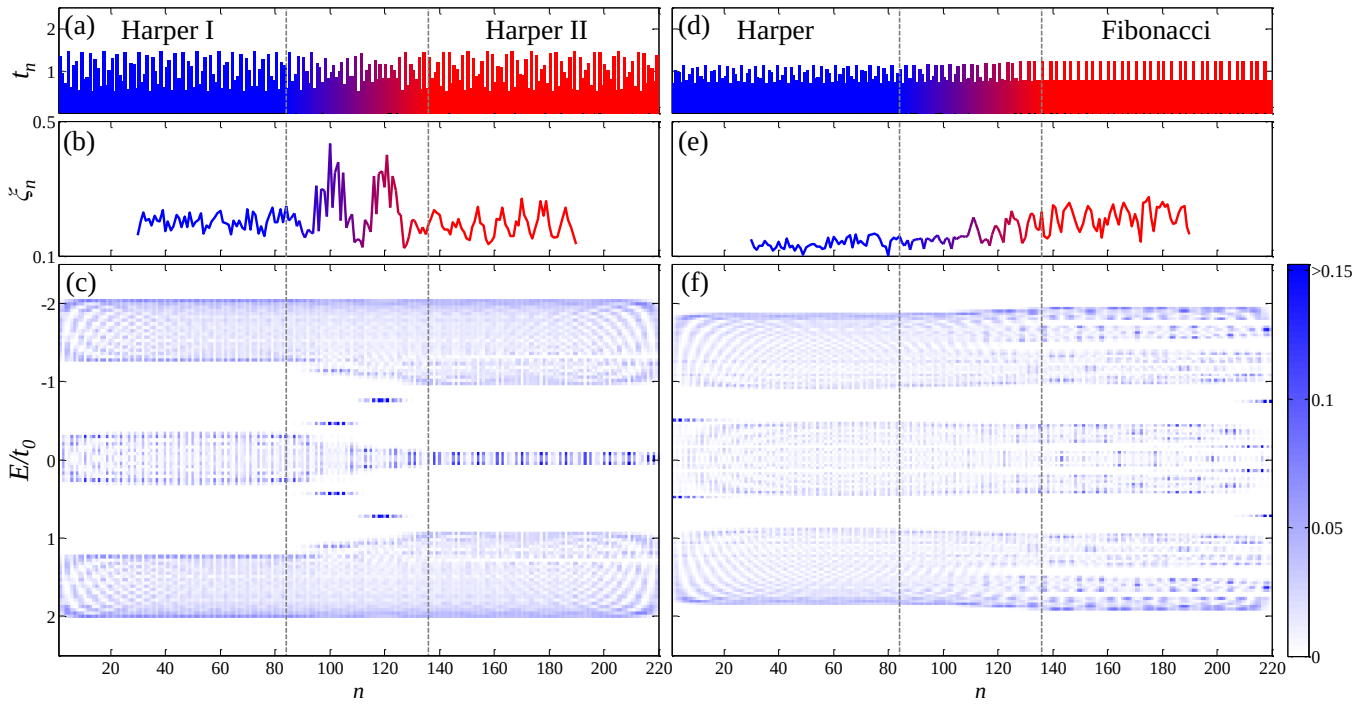

FIG. 2. (Color online) Summary of results for a smooth deformation between (a-c) two topologically inequivalent Harper QCs, and (d-f) topologically equivalent Harper and Fibonacci QCs. In both experiments, $L_I = 84$ (blue), $L_{II} = 84$ (red) and $L_D = 51$ (purple hues). (a) The hopping amplitude t_n as a function of the lattice site n, for modulation frequencies $b_I = 2/(1+\sqrt{5})$ and $b_{II} = 2/(1+\sqrt{6.5})$ of the Harper QCs. (b) Experimentally-measured ξ_n for $\Delta = 7$, as a function of the injection site n. The two peaks within the deformation region imply the existence of localized states. (c) Numerically obtained LDOS of the structure, $D_n(E)$. The energy bands are composed of extended states, while localized states (roughly 15 sites wide) traverse the gaps in the deformation region. These states manifest the transition between the inequivalent QCs. (d-f) Same as (a-c), but with a Harper QC deformed into a Fibonacci QC with $b_I = (\tau_{II}+1)/\tau_{II} = 2/(1+\sqrt{5})$. Here, ξ_n shows no sign of localized states. Accordingly, though the distribution of the bands changes along the structure, no energy gap is closed. This proves the equivalence between the two QCs.

showing no sign of localized states within the deformation region. The numerically obtained LDOS is shown in Fig. 2(f). While the configuration of the bands changes considerably between the two QCs, no gap is closed along the deformation. Note, also, that two subgap states appear at the sharp boundaries with the vacuum [40]. The open gaps and the corresponding absence of peaks in ξ_n serves as experimental evidence of the equivalence between the Fibonacci and the Harper QCs.

To conclude, in this paper we have presented a novel method to study topological phase transitions using a continuous deformation between two systems, which acts as a smooth boundary between them. When the boundary is sufficiently smooth, observations of subgap states localized within the deformation area serve as evidence of the phase transition. Such subgap states do not appear when a phase transition does not take place, namely between topologically equivalent systems. Our method extends the prevailing approach which focuses on states that appear at sharp boundaries between topologically-nontrivial systems and the vacuum. It has proven useful in studying the topological characterization of 1D quasiperiodic systems, since it circumvents the subtlety of their boundary phenomena at sharp boundaries. Furthermore, this technique may be useful to study other topological systems, such as (i) the weak and the crystalline topological insulators, where the surface breaks the underlying symmetry [42–44]; (ii) varying dopant concentration in 3D topological insulators [45]; and (iii) nanowires that may host Majorana fermions at their boundaries [8–10].

We thank Y. Avron, R. Lifshitz, A. Keselman and S. Huber for fruitful discussions. We thank the U.S. Israel Binational Science Foundation, the Minerva Foundation of the DFG, Crown Photonics Center, and ISF Grant No. 700822030182 for financial support.

[1] M. Z. Hasan and C. L. Kane, Rev. Mod. Phys. **82**, 3045 (2010).
[2] X.-L. Qi and S.-C. Zhang, Rev. Mod. Phys. **83**, 1057 (2011).
[3] K. von Klitzing, G. Dorda, and M. Pepper, Phys. Rev. Lett. **45**, 494 (1980).
[4] M. König, S. Wiedmann, C. Brne, A. Roth, H. Buhmann, L. W. Molenkamp, X.-L. Qi, and S.-C. Zhang, Science **318**, 766 (2007).
[5] D. Hsieh, D. Qian, L. Wray, Y. Xia, Y. S. Hor, R. J.

Cava, and M. Z. Hasan, Nature **452**, 970 (2008).
[6] Y. Xia, D. Qian, D. Hsieh, L. Wray, A. Pal, H. Lin, A. Bansil, D. Grauer, Y. S. Hor, R. J. Cava, et al., Nature Phys. **5**, 398 (2009).
[7] H. Zhang, C. X. Liu, X. L. Qi, X. Dai, Z. Fang, and S. C. Zhang, Nature Phys. **5**, 438 (2009).
[8] V. Mourik, K. Zuo, S. M. Frolov, S. R. Plissard, E. P. A. M. Bakkers, and L. P. Kouwenhoven, Science **336**, 1003 (2012).
[9] M. T. Deng, C. L. Yu, G. Y. Huang, M. Larsson, P. Caroff, and H. Q. Xu (2012), arXiv:1204.4130.
[10] A. Das, Y. Ronen, Y. Most, Y. Oreg, M. Heiblum, and H. Shtrikman (2012), arXiv:1205.7073.
[11] Z. Wang, Y. Chong, J. D. Joannopoulos, and M. Soljačić, Nature **461**, 772 (2009).
[12] T. Kitagawa, M. A. Broome, A. Fedrizzi, M. S. Rudner, E. Berg, I. Kassal, A. Aspuru-Guzik, E. Demler, and A. G. White, Nature Comm. **3**, 882 (2012).
[13] N. Goldman, I. Satija, P. Nikolic, A. Bermudez, M. A. Martin-Delgado, M. Lewenstein, and I. B. Spielman, Phys. Rev. Lett. **105**, 255302 (2010).
[14] Y. E. Kraus, Y. Lahini, Z. Ringel, M. Verbin, and O. Zilberberg, Phys. Rev. Lett. **109**, 106402 (2012).
[15] Y. E. Kraus and O. Zilberberg, Phys. Rev. Lett. **109**, 116404 (2012).
[16] P. G. Harper, Proc. Phys. Soc. London A **68**, 874 (1955).
[17] S. Aubry and G. André, Ann. Isr. Phys. Soc. **3**, 133 (1980).
[18] M. Kohmoto, L. P. Kadanoff, and C. Tang, Phys. Rev. Lett. **50**, 1870 (1983).
[19] S. Ostlund, R. Pandit, D. Rand, H. J. Schellnhuber, and E. D. Siggia, Phys. Rev. Lett. **50**, 1873 (1983).
[20] J. H. Han, D. J. Thouless, H. Hiramoto, and M. Kohmoto, Phys. Rev. B **50**, 11365 (1994).
[21] M. Kohmoto, B. Sutherland, and C. Tang, Phys. Rev. B **35**, 1020 (1987).
[22] F. Mei, S.-L. Zhu, Z.-M. Zhang, C. H. Oh, and N. Goldman, Phys. Rev. A **85**, 013638 (2012).
[23] Z. Xu, L. Li, and S. Chen (2012), arXiv:1210.7696.
[24] M. Tezuka and N. Kawakami, Phys. Rev. B **85**, 140508 (2012).
[25] O. Viyuela, A. Rivas, and M. A. Martin-Delgado (2012), arXiv:1207.2198.
[26] W. DeGottardi, D. Sen, and S. Vishveshwara (2012), arXiv:1208.0015.
[27] X. Cai, L.-J. Lang, S. Chen, and Y. Wang (2012), arXiv:1208.2532.
[28] I. I. Satija and G. G. Naumis (2012), arXiv:1210.5159.
[29] D. N. Christodoulides, F. Lederer, and Y. Silberberg, Nature **424**, 817 (2003).
[30] F. Lederer, G. I. Stegeman, D. N. Christodoulides, G. Assanto, M. Segev, and Y. Silberberg, Physics Reports **463**, 1 (2008), ISSN 0370-1573.
[31] M. Ams, G. Marshall, P. Dekker, M. Dubov, V. Mezentsev, I. Bennion, and M. Withford, Selected Topics in Quantum Electronics, IEEE Journal of **14**, 1370 (2008).
[32] A. Szameit, D. Blömer, J. Burghoff, T. Schreiber, T. Pertsch, S. Nolte, A. Tünnermann, and F. Lederer, Opt. Express **13**, 10552 (2005).
[33] Note that the case of $\Delta = 0$ is the return probabilty, $\xi_n = |\psi_n|^2$. This generalization is required due to the finite width of subgap states.
[34] D. R. Hofstadter, Phys. Rev. B **14**, 2239 (1976).
[35] D. J. Thouless, M. Kohmoto, M. P. Nightingale, and M. den Nijs, Phys. Rev. Lett. **49**, 405 (1982).
[36] B. Grünbaum and G. C. Shephard, *Tilings and patterns* (W. H. Freeman & Co., New York, NY, USA, 1986), ISBN 0-716-71193-1.
[37] D. Levine and P. J. Steinhardt, Phys. Rev. Lett. **53**, 2477 (1984).
[38] H. Hiramoto and M. Kohmoto, Int. J. Mod. Phys. B **6**, 281 (1992).
[39] S. Jitomirskaya and C. Marx, Journal of Fixed Point Theory and Applications **10**, 129 (2011).
[40] See Supplemental Material for more details.
[41] To align the energy spectra of the Harper and Fibonacci QC, a constant shift is added to the hopping amplitude.
[42] Z. Ringel, Y. E. Kraus, and A. Stern, Phys. Rev. B **86**, 045102 (2012).
[43] L. Fu, Phys. Rev. Lett. **106**, 106802 (2011).
[44] L. Fu and C. Kane, arXiv:1208.3442 (2012).
[45] T. Sato, K. Segawa, K. Kosaka, S. Souma, K. Nakayama, K. Eto, T. Minami, Y. Ando, and T. Takahashi, Nat. Phys. **7**, 840 (2011).
[46] R. B. Laughlin, Phys. Rev. B **23**, 5632 (1981).
[47] J. Zak, Phys. Rev. Lett. **62**, 2747 (1989).
[48] Z. Ringel and Y. E. Kraus, Phys. Rev. B **83**, 245115 (2011).

SUPPLEMENTAL MATERIAL

I. EFFECT OF FINITE-SIZED DEFORMATION ON THE PHASE TRANSITION

In the main text, we study the phase transition that occurs when two topologically distinct quasicrystals (QCs) are deformed from one into the other, and its absence when the two QCs are topologically equivalent. This transition can be obtained by adiabatically deforming between the two QCs in real space, thereby creating a smooth boundary between them. As a result, when a topological phase transition occurs, the energy gap is continuously traversed by states localized within the deformation region. However, in physical systems, the deformation takes place over a finite length, making it not strictly adiabatic, and the gap closure is disrupted. Nevertheless, a finite number of subgap states remain, and their energies discretely traverse the gap. Here we show that these states serve as evidence of the topological phase transition, since their level spacing decreases with the deformation length.

Figure 3 depicts the numerically obtained local density of states (LDOS) for structures deforming between two topologically distinct Harper QCs. For this plot, the parameters are $b_I = 2/(1+\sqrt{5})$, $b_{II} = 2/(1+\sqrt{6.5})$, $\lambda_I = \lambda_{II} = 0.475$, $\phi_I = \phi_{II} = 0$, and $L_I + L_D + L_{II} = 460$. In Fig. 3(a), the deformation length is $L_D = 60$, and 3 subgap states appear within each one of the large gaps. In Fig. 3(b), $L_D = 300$, and 15 subgap states appear. As L_D increases, the number of subgap states within a gap (N_{sub}) increases, while the spacing between their energies (level spacing) decreases. Figure 4 plots the level spacing between two states residing in the middle of a large energy gap as a function of L_D. We can see that the level spacing scales as $\sim 1/L_D$. Therefore, in the limit of $L_D \to \infty$, we approach the continuous phase transition.

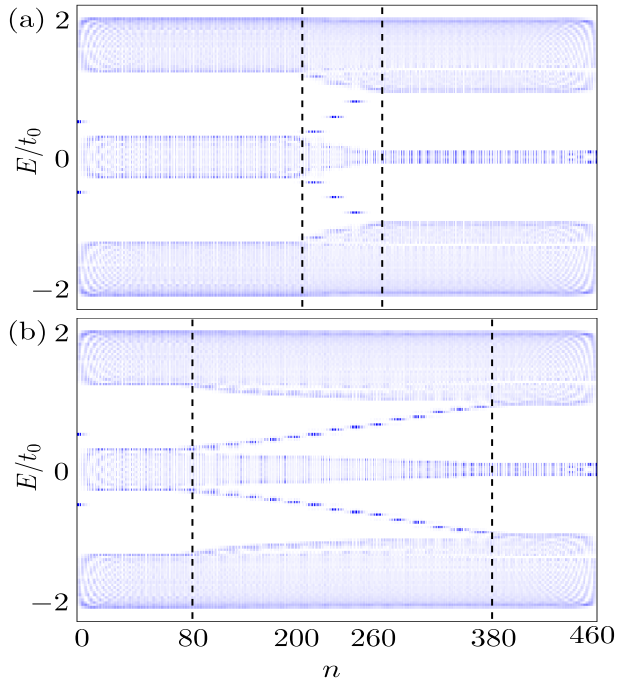

FIG. 3. Numerically obtained LDOS for deformation between inequivalent Harper QCs, with $b_I = 2/(1+\sqrt{5})$ and $b_{II} = 2/(1+\sqrt{6.5})$. (a) The deformation length is $L_D = 60$. The gap is traversed by 3 states in the deformation region. (b) For $L_D = 300$, there are 15 subgap states, and the level spacing between them decreases correspondingly.

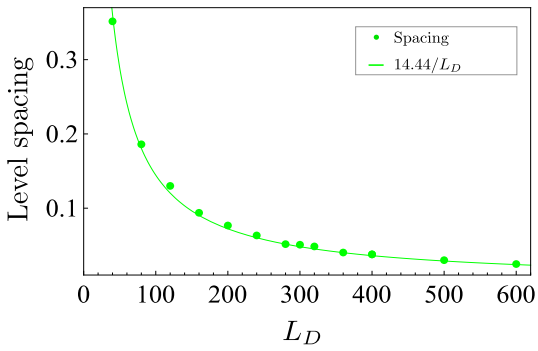

FIG. 4. Level spacing between two states in the middle of a large gap as a function of the deformation length L_D. While the width of the states (l_{sub}) is fixed, the number of states scales as L_D, and their level spacing scales as l_{sub}/L_D. The dots are numerically obtained data, and the fitted curve matches $14.44/L_D$.

The level spacing can be approximated by Δ/N_{sub}, where Δ is the size of the gap. The scaling of $1/L_D$ implies that there is an additional length scale, namely the width of the subgap states, l_{sub}. Given a fixed l_{sub}, the number of subgap states within the deformation region is approximately $N_{\text{sub}} \approx L_D/l_{\text{sub}}$, and their level spacing scales like l_{sub}/L_D. The width l_{sub} controls the smoothness of the boundary, and sets a lower bound on the deformation length for which subgap states always appear, i.e. $L_D > l_{\text{sub}}$. We can therefore conclude that structures with a finite deformation length larger than l_{sub} can indeed serve as a probe of the existence of a topological phase transition.

II. BOUNDARY STATES AT A SHARP BOUNDARY AND THE ROLE OF ϕ

We have seen that subgap states appear within a finite-length boundary between topologically inequivalent QCs. These states always appear for sufficiently long deformation regions ($L_D \gg l_{\text{sub}}$), and their number increases with the deformation length L_D.

In the opposite limit of $L_D \to 0$, the boundary becomes sharp. At a sharp boundary, subgap states may or may not appear, depending on the exact pattern of the QCs [14]. Recall that the Harper modulation [cf. Eq. (5)

in the main text] includes the parameter ϕ. This parameter shifts the origin of the quasiperiodic pattern, and is known as a phasonic degree of freedom. The appearance of subgap states at a sharp boundary with the vacuum is controlled by ϕ, since it determines the exact pattern of the QC at the termination point. As ϕ varies from 0 to 2π, boundary states continuously traverse the energy gaps. The number of gap-traversing states is given by the corresponding Chern number, which is determined by the modulation frequency b.

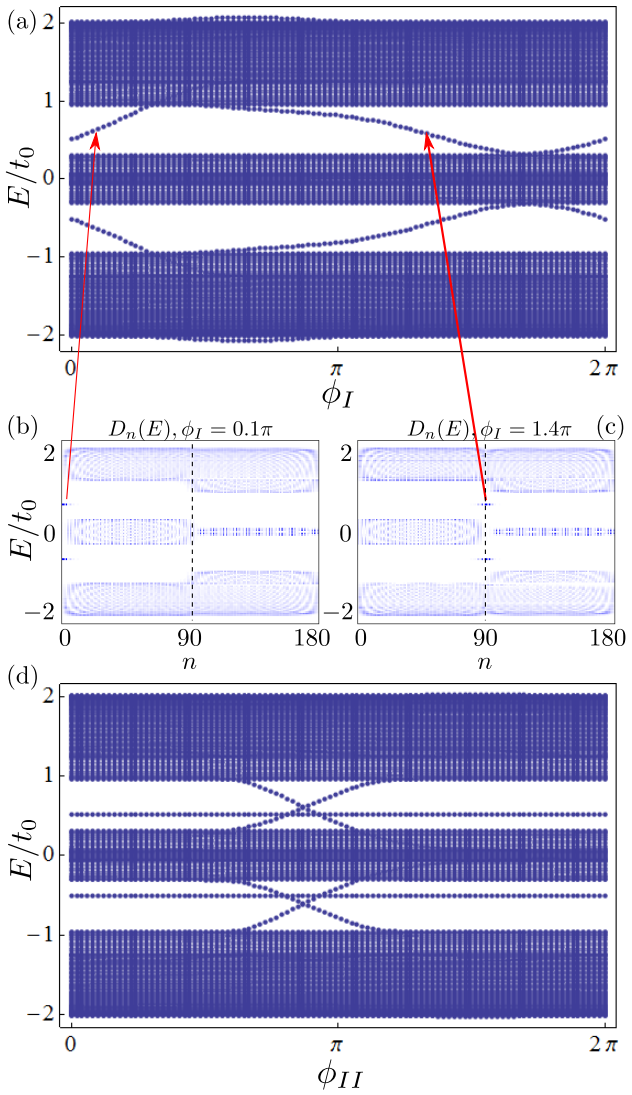

FIG. 5. Boundary states at a sharp boundary between two QCs. (a) Numerically obtained spectrum of a structure with the same parameters as in Fig. 3 and $L_D = 0$ as a function of ϕ_I. The large gaps are traversed by two states when ϕ_I is scanned from 0 to 2π. (b) The corresponding LDOS for $\phi_I = 0.1\pi$. The gap-traversing state is localized at the boundary of QC I with the vacuum. (c) The corresponding LDOS for $\phi_I = 1.4\pi$. The subgap state is localized at the sharp boundary between QC I and QC II. (d) The spectrum of the structure as a function of ϕ_{II}. Again, two states traverse the gaps, where one of them is localized at the boundary of QC II. The horizontal line in the middle of the gaps belongs the boundary state of QC I, which is unaffected by ϕ_{II}.

At a sharp boundary between two QCs, subgap states traverse the gap as either ϕ_I or ϕ_{II} is scanned. This can be seen in Figs. 5(a)-(d), which show the numerically obtained spectra of a structure with the parameters from the previous section and $L_D = 0$, as a function of ϕ_I and ϕ_{II}. As ϕ_I is scanned, two states traverse each one of the large gaps, one localized at the sharp boundary of QC I with the vacuum, and the other at the sharp boundary between QC I and QC II [as seen from the corresponding LDOS in Figs. 5(b) and 5(c)]. A similar behavior is observed when ϕ_{II} is scanned, only now, one of two the gap-traversing states is localized at the sharp boundary of QC II with the vacuum.

In contrast to a sharp boundary, for infinitely long L_D, the gap traversing states are independent of ϕ. For finite L_D, where there is a finite number of subgap states, the gap completely closes when ϕ is scanned. This can be seen in Fig. 6, which depicts a numerically obtained spectrum with $L_D = 80$ as a function of ϕ_I. As ϕ_I is scanned from 0 to 2π, the energy of each subgap state in the deformation region continuously connects to the energy of the next level. We can also recognize the state at the boundary of QC I with the vacuum [cf. Fig. 5(a)]. Notably, the motion of the eigenstates with ϕ_I represents pumping analogues to Laughlin's pumping in the integer quantum Hall effect [46–48].

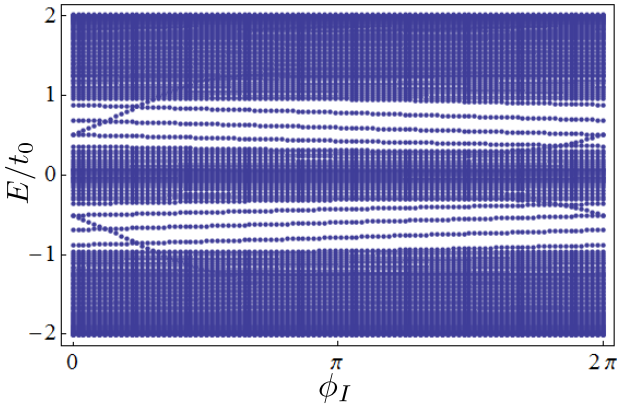

FIG. 6. Spectrum of a structure with the same parameters as in Fig. 3 and $L_D = 80$ as a function of ϕ_I. The energy of each subgap state in the deformation region approaches the energy of the next one when ϕ_I is scanned. The state at the boundary of QC I with the vacuum behaves like in Fig. 5(a).